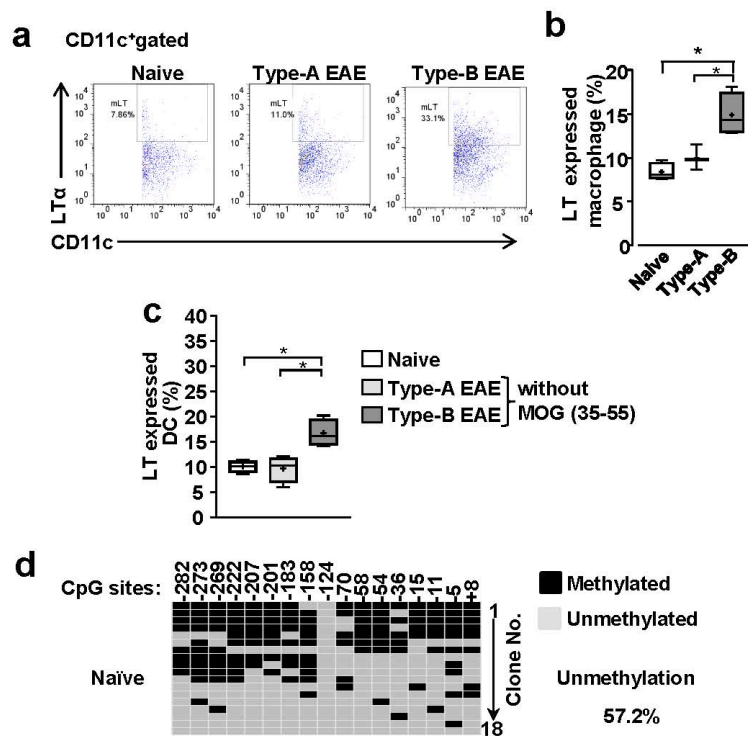


Supplementary Figure 1

EAE induced by several immunization methods and phenotypes on cell migration, demyelination and nociceptive sensitivity in mice with Type-A and Type-B EAE.

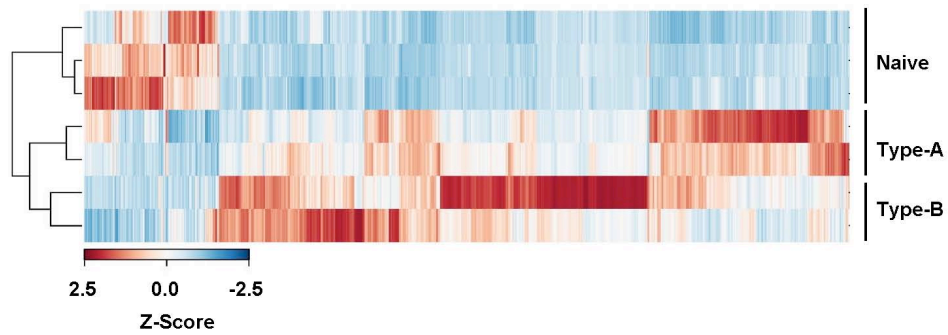
(a) EAE severity in *Nlrp3*^{-/-} mice was evaluated. EAE was induced with 6 different methods, as indicated in Online Methods. (b) AUC between 0 and 20-dpi. Method 1 (*n*=4), Method 2-6 (*n*=5). $P_{(Method\ 1\ vs\ 2)}=0.0006$, $t(7)=5.98$, $P_{(Method\ 1\ vs\ 3)}<0.0001$, $t(7)=12.54$, $P_{(Method\ 1\ vs\ 4)}=0.0027$, $t(7)=4.54$, $P_{(Method\ 1\ vs\ 5)}<0.0001$, $t(7)=8.15$, $P_{(Method\ 1\ vs\ 6)}<0.0001$, $t(7)=10.63$. (c) Numbers of total immune cells were evaluated in the brains and spinal cords (S.C.) of mice with Type-B EAE at 17-dpi. *n*=4. Brain: $P_{(WT\ vs\ Nlrp3^{-/-})}=0.8159$, $t(6)=0.2433$, $P_{(WT\ vs\ Asc^{-/-})}=0.5685$, $t(6)=0.6031$. Spinal cord: $P_{(WT\ vs\ Nlrp3^{-/-})}=0.5226$, $t(6)=0.6787$, $P_{(WT\ vs\ Asc^{-/-})}=0.8984$, $t(6)=0.1332$. (d) IFN β treatment on *Nlrp3*^{-/-} mice with Type-B EAE induced with Method 6. IFN β (3×10^4 unit/mouse) were *i.p.* injected every other day from day 0 to 8 as previously performed. (e) Time course on body weight change in Type-A and Type-B EAE. (f) *Il1b* mRNA levels in splenic DC from naive, Type-A, and Type-B EAE mice at 9 dpi. $P_{(Naive\ vs\ Type-A)}=0.0059$, $t(4)=5.344$, $P_{(Naive\ vs\ Type-B)}<0.0001$, $t(4)=18.55$, $P_{(Type-A\ vs\ Type-B)}=0.0004$, $t(4)=10.83$. (g,h) Levels of extracellular IL-1 β (f) and p20 caspase-1 (g) in 24h splenocyte culture supernatants (*n*=4 for Type-A, *n*=5 for Type-B). $P=0.0261$, $t(6)=2.724$ (g). $P=0.0020$, $t(6)=4.794$ (h). (i) Infiltrated cell numbers in the brain and spinal cord (*n*=7). Brain: $P_{(Total)}=0.0028$, $t(12)=3.747$, $P_{(CD4)}=0.018$, $t(12)=2.737$, $P_{(Th17)}=0.0167$, $t(12)=2.78$, $P_{(Th1)}=0.0165$, $t(12)=2.784$, $P_{(CD8)}=0.0329$, $t(12)=2.41$, $P_{(B)}=0.0013$, $t(12)=4.165$, $P_{(DC)}=0.0003$, $t(12)=5.008$, $P_{(PMN)}=0.0004$, $t(12)=4.912$, $P_{(Mac)}=0.0027$, $t(12)=3.759$. Spinal cord: $P_{(Total)}=0.0035$, $t(12)=3.621$, $P_{(CD4)}=0.0002$, $t(12)=5.372$, $P_{(Th17)}=0.0003$, $t(12)=4.997$, $P_{(Th1)}=0.00465$, $t(12)=2.221$, $P_{(CD8)}=0.0104$, $t(12)=3.032$, $P_{(B)}=0.0918$, $t(12)=1.833$, $P_{(DC)}=0.0429$, $t(12)=2.263$, $P_{(PMN)}=0.0011$, $t(12)=4.29$, $P_{(Mac)}=0.089$, $t(12)=1.849$. (j) Representative LFB-stained images of brains at 17-dpi. Red arrows indicate reduced LFB intensity, *i.e.*, reduced myelin. Scale bars, 200 μ m. (k) T2 FLAIR MRI analysis of spinal cords obtained from mice at 18-dpi. Yellow arrows indicate areas of potential myelin loss. (l) Thermal sensitivity evaluated by a hot-plate test in 9-dpi mice, which did not show any EAE symptoms and motor dysfunction. *n*=8. $P_{(Naive\ vs\ Type-A)}=0.1524$, $t(14)=1.514$, $P_{(Naive\ vs\ Type-B)}=0.0013$, $t(14)=4.026$, $P_{(Type-A\ vs\ Type-B)}=0.0217$, $t(14)=2.582$. *: $p<0.05$. All statistical analyses in this figure were performed by two-tailed unpaired Student's *t*-test. All the experimental data and images are representatives from at least 2 similar experiments for each.



Supplementary Figure 2

mLT expression on DC.

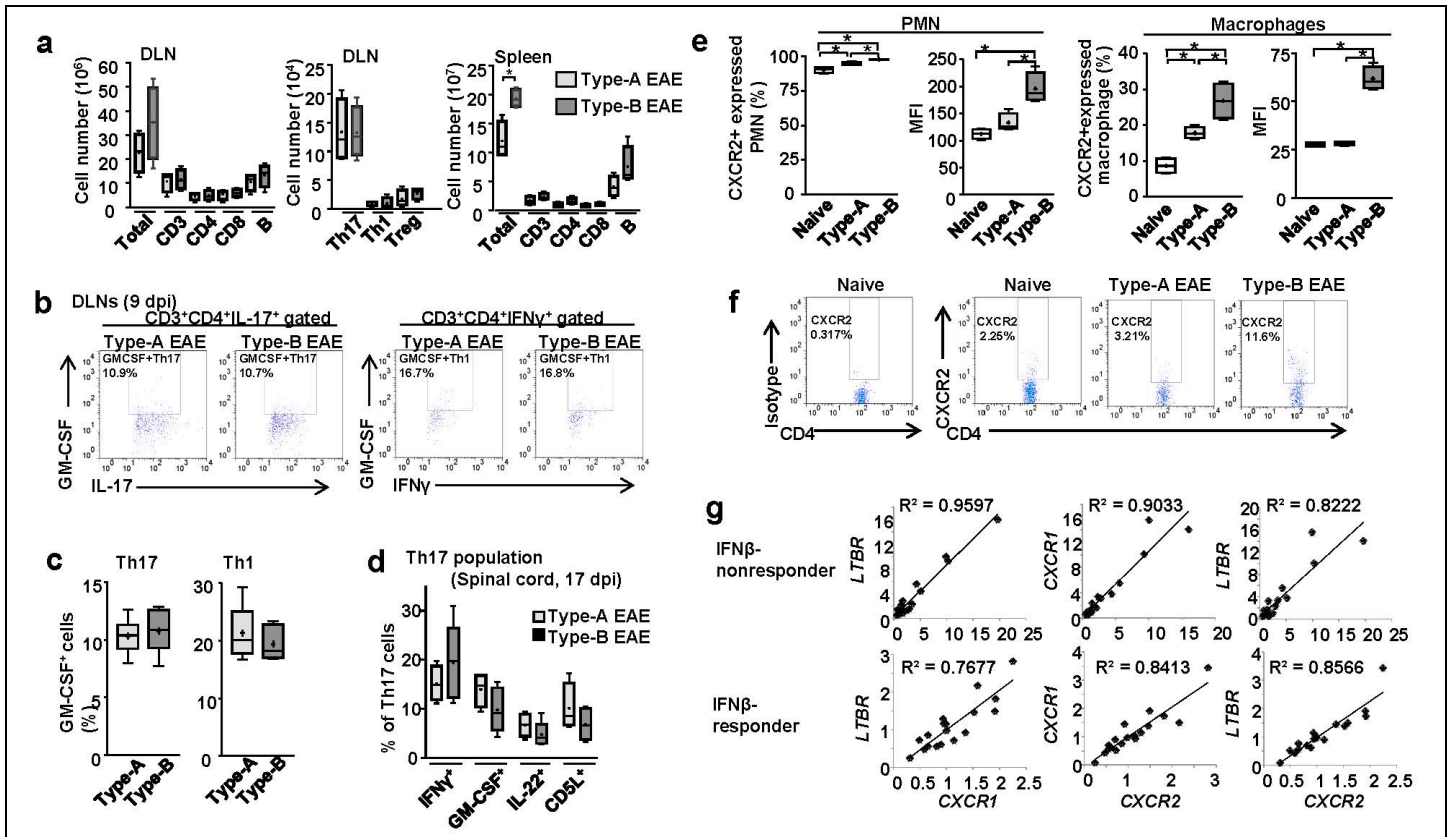
(a) Flow charts showing mLT expression in DC (CD11c⁺ gated) obtained from naïve mice, Type-A EAE mice, and Type-B EAE mice at 9-dpi. (b) Percentages of LTα⁺ (i.e., mLT⁺) macrophages, determined by flow cytometry, in DLNs of naïve mice or mice with EAE at 9-dpi. Naïve (n=4), Type-A (n=3), Type-B (n=4). $P_{(Naive\ vs\ Type-A)}=0.1340$, $t(5)=1.7887$, $P_{(Naive\ vs\ Type-B)}=0.0024$, $t(6)=45.021$, $P_{(Type-A\ vs\ Type-B)}=0.0268$, $t(5)=3.101$, by two-tailed unpaired Student's *t*-test. (c) Evaluating mLT expression on DCs from mice received CFA injection alone without MOG. One group received 200 µg *Mtb* in CFA (*Mtb* dosage for Type-A EAE), and another group had 400 µg *Mtb* in CFA twice (*Mtb* dosage for Type-B EAE). (n=6) $P_{(Naive\ vs\ Type-A)}=0.07939$, $t(6)=0.2732$, $P_{(Naive\ vs\ Type-B)}=0.0040$, $t(6)=4.519$, $P_{(Type-A\ vs\ Type-B)}=0.0095$, $t(6)=3.748$, by two-tailed unpaired Student's *t*-test. (d) Methylation analysis was carried out by bisulfite conversion on the *Lta* promoter in DCs from naïve mice. Methylated and unmethylated CpG were shown with black and gray boxes, respectively



Supplementary Figure 3

RNA-seq analysis.

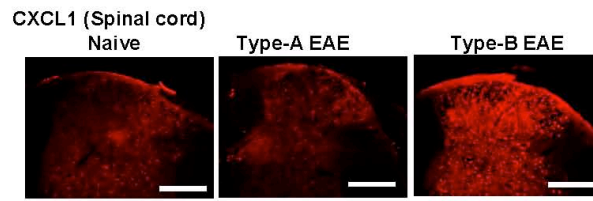
Heatmap for differentially expressed genes in CD4⁺ T cells isolated from naïve, Type-A EAE mice, and Type-B EAE mice at 9-dpi. Genes and samples have been clustered using correlation distance with complete linkage. A gene is listed on the heatmap if it had a p-value ≤ 0.05 and a $\log_2FC > 1$ or < -1 .



Supplementary Figure 4

Comparison of IFN β -responders and non-responders in mouse EAE and human RRMS.

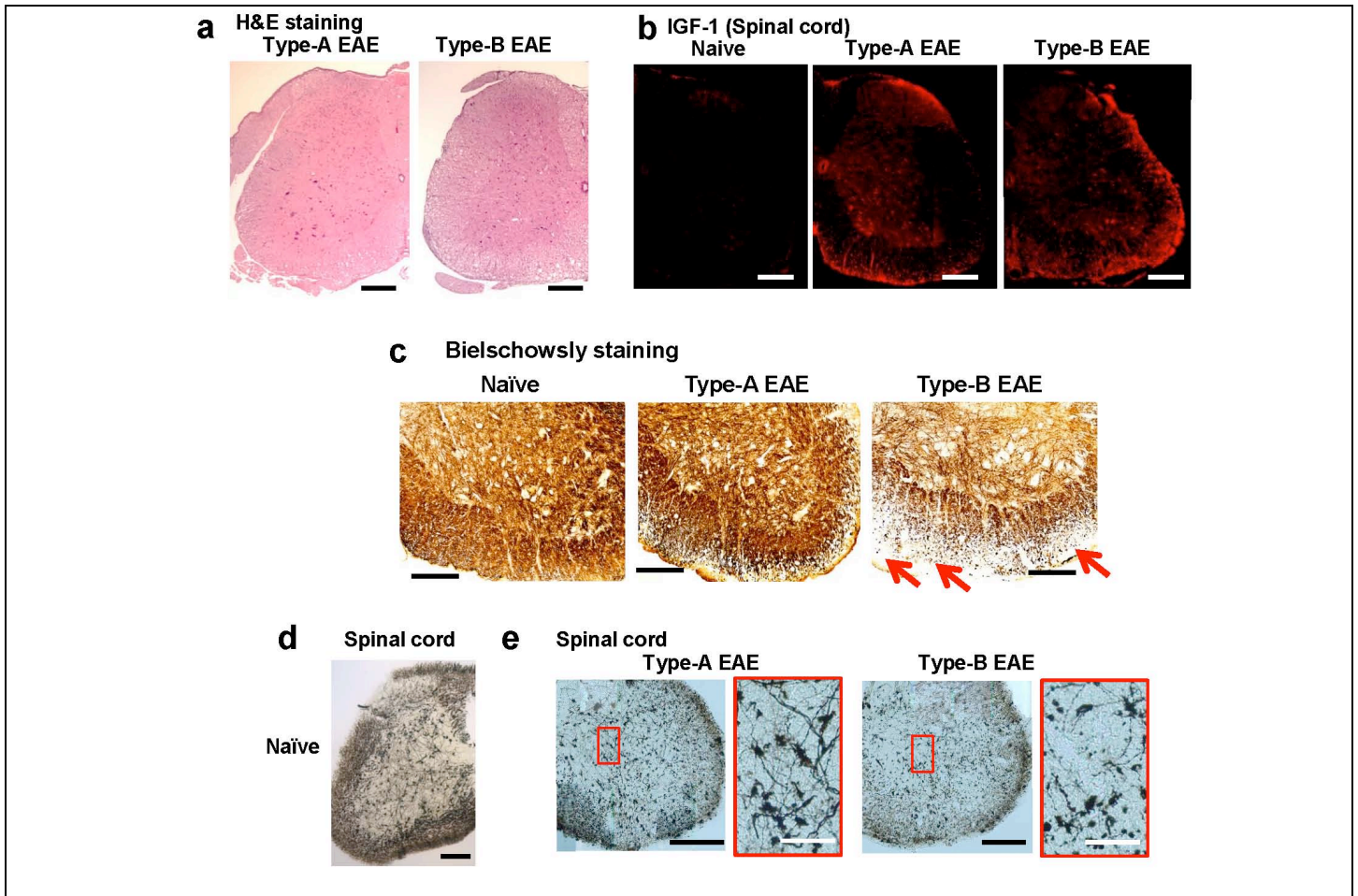
(a) Numbers of indicated cell types obtained from DLNs and spleen on 17-dpi were evaluated between Type-A and Type-B EAE. $n=4$. DLNs: $P_{(Total)}=0.2073$, $t(6)=1.413$, $P_{(CD3)}=0.8466$, $t(6)=0.202$, $P_{(CD4)}=0.9285$, $t(6)=0.09353$, $P_{(CD8)}=0.7413$, $t(6)=0.3459$, $P_{(B)}=0.4141$, $t(6)=0.8773$, $P_{(Th17)}=0.9724$, $t(6)=0.03605$, $P_{(Th1)}=0.9017$, $t(6)=0.1289$, $P_{(Treg)}=0.3556$, $t(6)=1.001$. Spleen: $P_{(Total)}=0.0072$, $t(6)=3.99$, $P_{(CD3)}=0.2537$, $t(6)=1.262$, $P_{(CD4)}=0.1781$, $t(6)=1.525$, $P_{(CD8)}=0.3999$, $t(6)=0.906$, $P_{(B)}=0.1371$, $t(6)=1.715$. (b, c) Representative flow charts (b) and proportion (c) for GM-CSF-producing Th1 and Th17 cells from Type-A and Type-B EAE at 9-dpi. $n=6$. Th17: $P=0.6568$, $t(10)=0.4579$, Th1: $P=0.3954$, $t(10)=0.8879$. (d) Proportion for IFN γ ⁻, GM-CSF⁻, IL-22⁻ producing and CD5L⁻ expressing Th17 cells in spinal cords from Type-A and Type-B EAE mice at 17-dpi. Type-A ($n=4$), Type-B ($n=5$). $P_{(IFN\gamma)}=0.3493$, $t(7)=1.0037$, $P_{(GM-CSF)}=0.1760$, $t(7)=1.505$, $P_{(IL-22)}=0.2859$, $t(7)=1.155$, $P_{(CD5L)}=0.2641$, $t(7)=1.214$. (e) Proportions and MFI of CXCR2⁺ neutrophils and macrophages obtained from naïve mice and mice with either Type-A or Type-B EAE at 9-dpi. $n=4$. PMN %: $P_{(Naive vs Type-A)}=0.0102$, $t(6)=3.695$, $P_{(Naive vs Type-B)}=0.0004$, $t(6)=7.001$, $P_{(Type-A vs Type-B)}=0.0022$, $t(6)=5.131$. PMN MFI: $P_{(Naive vs Type-A)}=0.0777$, $t(6)=2.125$, $P_{(Naive vs Type-B)}=0.0014$, $t(6)=5.588$, $P_{(Type-A vs Type-B)}=0.0090$, $t(6)=3.81$. Macrophage %: $P_{(Naive vs Type-A)}=0.0005$, $t(6)=6.774$, $P_{(Naive vs Type-B)}=0.0006$, $t(6)=6.48$, $P_{(Type-A vs Type-B)}=0.0161$, $t(6)=3.314$. Macrophage MFI: $P_{(Naive vs Type-A)}=0.33$, $t(6)=1.06$, $P_{(Naive vs Type-B)}=0.0001$, $t(6)=11.11$, $P_{(Type-A vs Type-B)}=0.0001$, $t(6)=10.89$. (f) Flow cytometry results showing CXCR2 protein expression on the CD4⁺ T surface in each group (naïve mice, Type-A, or Type-B EAE mice at 9-dpi). (g) Comparison of relative gene expression levels between *Ltbr* and *Cxcr1*, *Cxcr1* and *Cxcr2*, *Ltbr* and *Cxcr2*, normalized to *Vcam1* expression. Total PBMCs from IFN β -responder and non-responder RRMS patients were compared. All statistical analyses in this figure were performed by two-tailed unpaired Student's *t*-test. All the experimental data sets, except for (g), are representatives from at least 2 similar experiments for each.



Supplementary Figure 5

CXCL1 expression in spinal cords. .

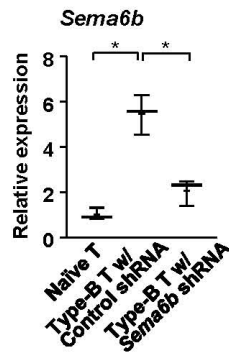
Shown are representative images of typical CXCL1 staining in spinal cords from naïve mice and mice with either Type-A or Type-B EAE at 9-dpi. Scale bars, 200 μ m. Images are representatives from 3 similar experiments.



Supplementary Figure 6

Histology of spinal cords in mice with Type-A or Type-B EAE.

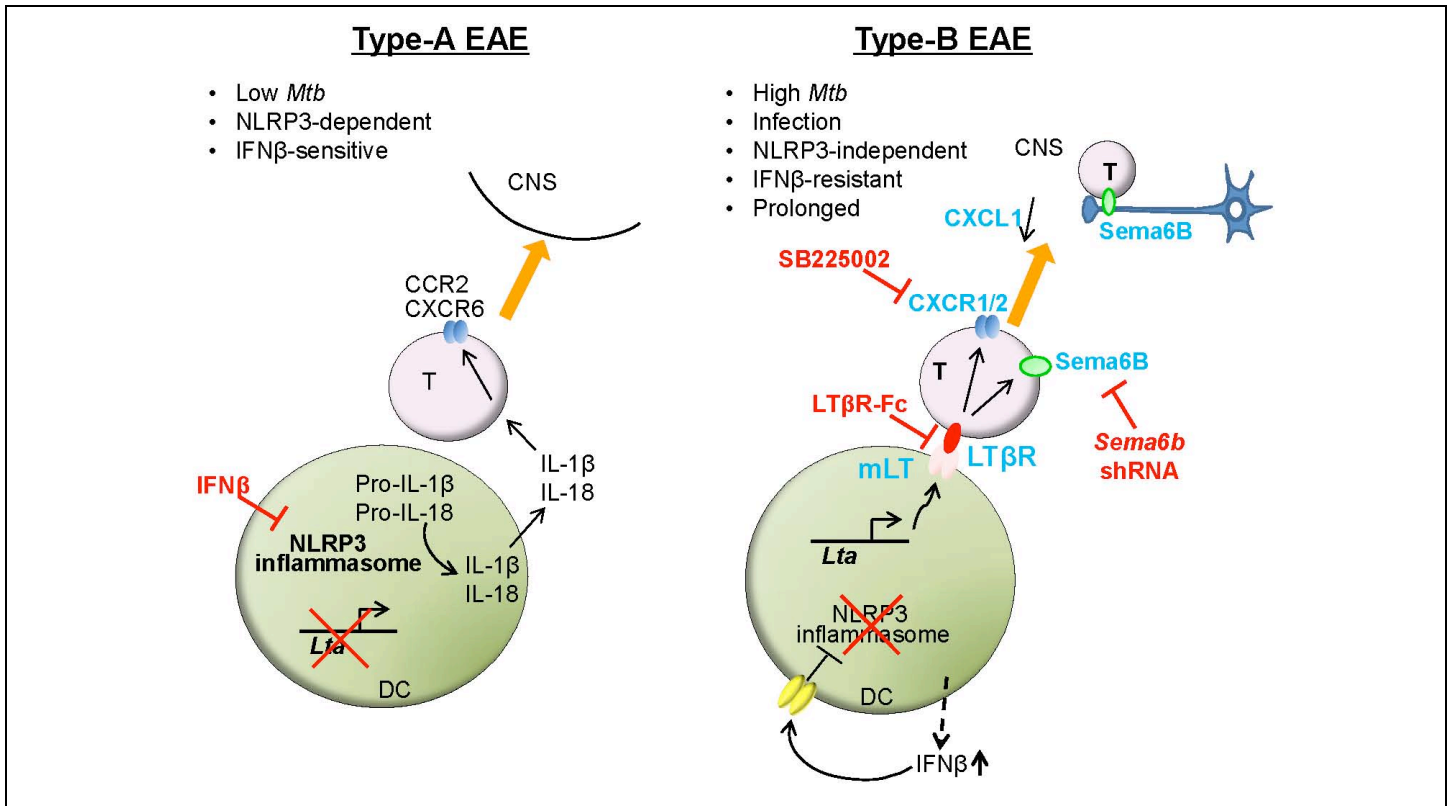
(a-e) Shown are representative images of typical staining from multiple mice. (a) H/E staining in the spinal cord of Type-A and Type-B EAE mice at 70-dpi. (b) IGF-1 staining in spinal cord of naïve mice and mice with either Type-A or Type-B EAE at 22-dpi. (c) Bielschowsky neuron staining in spinal cords of naïve mice (e), and Type-A and Type-B EAE at 30-dpi. Red arrows indicate area showing reduced staining intensity in the spinal cord. (d,e) Golgi's silver staining in spinal cord of naïve mice (d), and Type-A and Type-B at 22-dpi (e). All scale bars in this figure except magnified figure in (e), 200 µm. All scale bars in magnified figure in (e), 50 µm. All images are representatives from 3 similar experiments.



Supplementary Figure 7

Sema6b shRNA knock-down in T cells. .

Sema6b expression levels in CD4⁺ T cells isolated from naïve or Type-B EAE mice at 9-dpi were evaluated by qPCR. *Sema6b* was knocked down by shRNA in the indicated group of CD4⁺ T cells. Control shRNA (scrambled shRNA sequence) was used for the control group. Values shown are obtained from three independent trials using one mouse per each. $n=3$. $P_{(Naïve\ T\ vs\ Type-B\ T+Control\ shRNA)}=0.0011$, $t(4)=8.396$, $P_{(Type-B\ T+Control\ shRNA\ vs\ Type-B\ T+Sema6b\ shRNA)}=0.0051$, $t(4)=5.559$. *: $p<0.05$.



Supplementary Figure 8

Schematic diagram of distinct pathology between two EAE subtypes. .

Type-A EAE is NLRP3 inflammasome-dependent and IFN β -sensitive. Type-B EAE is induced by immunization with higher doses of *Mtb* than Type-A EAE induction, and is NLRP3 inflammasome-independent and IFN β -resistant. Type-B EAE can also be induced with Type-A EAE induction methods with MHV68 infection or with rLT (rLT α 2 β 1) injection. In Type-B EAE, *Lta* gene expression is epigenetically induced in DCs and the expression of membrane-bound LT (mLT) on DCs are enhanced. mLT stimulate LT β R on CD4⁺ T cells, resulting in the upregulation of CXCR2 on CD4⁺ T cells. Blockade of LT β R (with LT β R-Fc) and CXCR2 (with SB225002) selectively inhibits the Type-B EAE progression. mLT is also involved in the induction of Sema6B in T cells. Sema6B causes neural damages, and this may be a reason for the prolonged and minimal remission in Type-B EAE.